

# Microwave Makes Carbon Nanotubes Less Defective

Wei Lin,<sup>†,\*</sup> Kyoung-Sik Moon,<sup>†</sup> Shanju Zhang,<sup>‡</sup> Yong Ding,<sup>†</sup> Jintang Shang,<sup>§</sup> Mingxiang Chen,<sup>⊥</sup> and Ching-ping Wong<sup>†,\*</sup>

<sup>†</sup>School of Materials Science and Engineering, Georgia Institute of Technology, 771 Ferst Drive NW, Atlanta, Georgia 30332, <sup>‡</sup>School of Polymer Textile and Fiber Engineering, Georgia Institute of Technology, 801 Ferst Drive NW, Atlanta, Georgia 30332, <sup>§</sup>Key Lab of MEMS of Education Ministry, Southeast University, Nanjing 210096, People's Republic of China, and <sup>⊥</sup>Wuhan National Laboratory for Optoelectronics, Huazhong University of Science and Technology, Wuhan 430074, People's Republic of China

**ABSTRACT** An ultrafast microwave annealing process has been developed to reduce the defect density in vertically aligned carbon nanotubes (CNTs). Raman and thermogravimetric analyses have shown a distinct defect reduction in the CNTs annealed in microwave for 3 min. Fibers spun from the as-annealed CNTs, in comparison with those from the pristine CNTs, show increases of ~35% and ~65%, respectively, in tensile strength (~0.8 GPa) and modulus (~90 GPa) during tensile testing; an ~20% improvement in electrical conductivity (~80000 S m<sup>-1</sup>) was also reported. The mechanism of the microwave response of CNTs was discussed.

**KEYWORDS:** carbon nanotube · microwave · defect · mechanical properties · electrical conductivity

Carbon nanotubes (CNTs) exhibit impressive potentials in many applications such as electrical interconnects,<sup>1–5</sup> thermal interface materials,<sup>6–10</sup> high-performance fibers,<sup>11–17</sup> and so on. Although the theoretical intrinsic electrical, thermal, and mechanical properties of an individual CNT are extraordinary,<sup>18</sup> synthesized CNTs in reality are far from being defect-free. Presence of structural defects in a CNT has been found to shadow its promise in real-life applications.<sup>19–28</sup> Defect reduction is the key to realizing the true potential of individual CNTs. Conventionally a high-temperature thermal annealing process is needed for CNT defect reduction. For example, annealing of single-walled carbon nanotubes (SWNTs) is usually carried out above 1200 °C in vacuum.<sup>29</sup> Although such annealing is effective in reducing SWNT defects, coalescence/reconstruction of SWNTs during high-temperature annealing has been found from time to time.<sup>30</sup> For multi-walled carbon nanotubes (MWNTs), a higher annealing temperature (typically above 1900 °C) is needed.<sup>22,31–33</sup> However, for on-substrate applications of vertically aligned MWNTs (VACNTs), for example, as thermal interface materials in electronic

packaging and for dry spinning of CNT fibers, the high-temperature thermal annealing process is not feasible because the commonly used growth substrates such as silicon and copper cannot sustain such high temperatures for such long duration. In some cases, degradation in mechanical properties was found for high-temperature annealed MWNTs.<sup>33</sup> Moreover, thermal annealing is too time-consuming and costly. Therefore, finding an alternative way to fast-anneal VACNTs has become significant. Recently, CNTs have been found to display strong microwave absorption accompanied by a rapid temperature increase to above 1550 °C.<sup>34–36</sup> The strong microwave absorption by CNTs has recently attracted considerable interest for both theoretical research and potential applications,<sup>35–40</sup> especially for CNT functionalizations,<sup>41–49</sup> the mechanism being still open to question though. In the present study, we report the application of microwave radiation for VACNT fast annealing; the annealed CNTs show great improvements in mechanical and electrical properties. What happens to CNT structure in microwave radiation and the mechanism of CNT response to microwave are discussed.

## RESULTS AND DISCUSSION

VACNT arrays of 1 mm thick were synthesized by the CVD process reported previously.<sup>5,50–52</sup> The influence of microwave radiation on the VACNTs was studied by investigating the Raman spectra (LabRAM ARAMIS, Horiba Jobin Yvon, with a 532-nm-wavelength laser) of the annealed VACNT samples under various microwave power outputs and duration. Raman scattering is a well-accepted characterization method for evaluating the degree of struc-

\*Address correspondence to cp.wong@mse.gatech.edu.

Received for review November 13, 2009 and accepted February 5, 2010.

Published online February 17, 2010.  
10.1021/nn901621c

© 2010 American Chemical Society

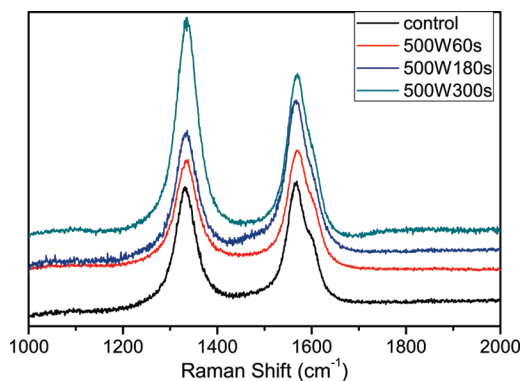


**Figure 1.** A selected regime of the typical Raman spectra of the control VACNT sample and the VACNT samples treated by VFM with 500 W of power at varied duration.

tural order of MWNTs, by using the ratio of the integrated intensity of D band ( $I_D$ ) at  $\sim 1334\text{ cm}^{-1}$  to that of G band ( $I_G$ ) at  $\sim 1570\text{ cm}^{-1}$ .<sup>53</sup> Also investigated is the ratio of the integrated intensity of D' band ( $I_{D'}$ , by least-squares fitting Lorentzian line shapes to the asymmetric G band in the spectra) at  $\sim 1610\text{ cm}^{-1}$  to  $I_G$ .<sup>54,55</sup> Figure 1 shows the typical Raman spectra (in a selective shift regime) of the control VACNT sample and the VACNT samples treated by VFM; the corresponding  $I_D/I_G$  and  $I_{D'}/I_G$  are shown in Figure 2.

It is evident that within short duration (*i.e.*,  $<180\text{ s}$ ) of microwave radiation,  $I_D/I_G$  and  $I_{D'}/I_G$  decrease with increased duration, indicating an improvement in the structural order of the microwave-annealed CNTs. We postulate that what happens during the microwave

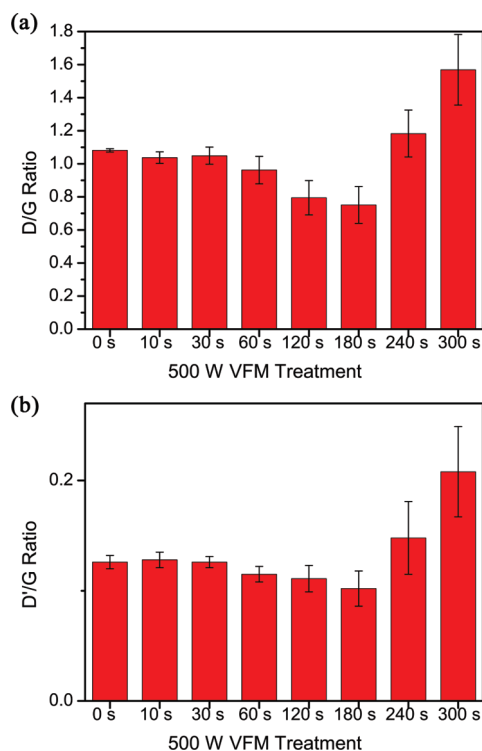


**Figure 2.**  $I_D/I_G$  (a) and  $I_{D'}/I_G$  (b) of the control VACNT sample and the VACNT samples treated by VFM with 500 W of power at varied duration.

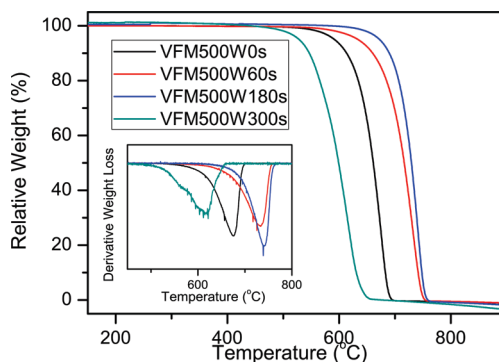


**Figure 3.** TGA results of the control VACNTs and VFM treated VACNTs; inset is the derivative weight loss plot against temperature.

annealing process is that the defective sites on the synthesized CNTs reconstruct to form graphitic structure, leading to the reduced  $I_D/I_G$  and  $I_{D'}/I_G$ . With extended microwave radiation duration,  $I_D/I_G$  and  $I_{D'}/I_G$  rise probably because of CNT degradation in microwave or because of CNT oxidation given that a highly effective argon protection is difficult to achieve in the VFM chamber.<sup>34</sup>

Our postulation can be verified by thermogravimetric analysis (TGA) of the VACNTs (Figure 3). TGA has been used widely to study the oxidative stability of CNTs so as to evaluate CNT quality, that is, defect density and purity.<sup>31,32,56,57</sup> In our study, TGA measurements were carried out in air, using a heating rate of  $10\text{ °C min}^{-1}$ , up to  $900\text{ °C}$ . For the control VACNTs, the temperature where the derivative weight loss peaks is  $\sim 675\text{ °C}$ , consistent with the reported values for defective (raw, unannealed) CNTs.<sup>31,56,58</sup> VFM (500 W) treatments of 1 and 3 min shift the peak temperature up to  $\sim 730\text{ °C}$  and  $\sim 740\text{ °C}$ , respectively, indicating an effective improvement in oxidative stability, comparable to high-temperature annealed CNTs.<sup>31</sup> In comparison, a 5-min treatment causes a dramatic structural instability. The TGA results show no detectable amorphous carbon or catalyst residue, indicating high purity of our synthesized VACNTs; therefore, the oxidative stability is a reflection of the crystalline defect density of the CNT structure. Increased defect density leads to increased local reactivity to oxygen and, consequently, a lower oxidative stability. Therefore, relatively short microwave radiation duration is effective in reducing the defect density of the VACNTs, while extended duration degrades the VACNTs by introducing more defects.

Further proof comes from X-ray photoelectron spectroscopy (XPS) investigations (SSX-100, Al K $\alpha$  source). XPS results in Figure 4 show the change in the oxygen signal from the VACNTs. Increased oxygen content on the CNT surface due to extended microwave duration is evident. However, not observed is any distinct difference in oxygen content between the control sample and the shortly treated sample, probably due to the limited sensitivity of XPS; the same for the high-resolution

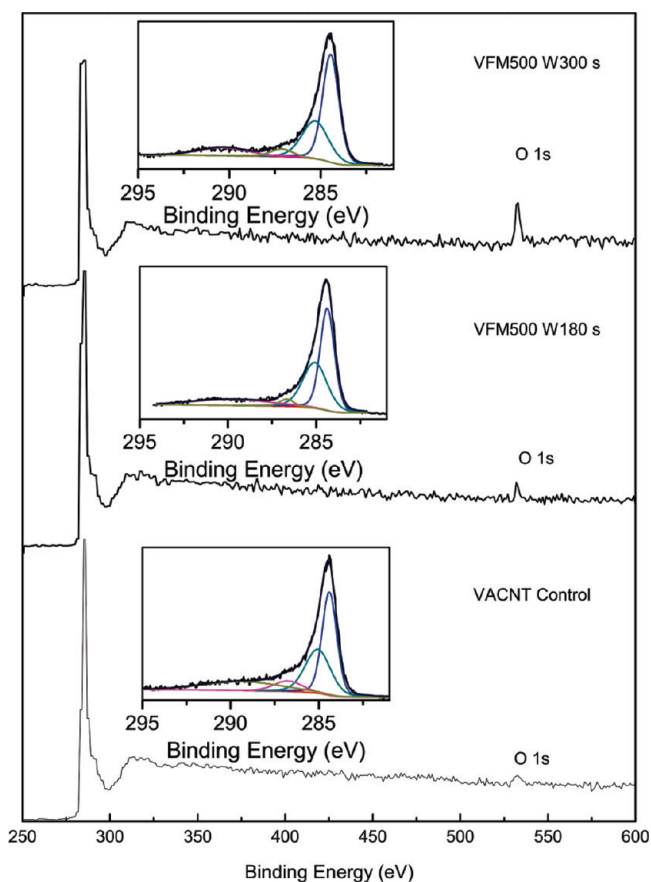


**Figure 4.** XPS surveys of the control VACNTs and the VFM treated VACNTs; insets are the corresponding high-resolution  $C_{1s}$  spectra.

spectra. High-resolution transmission electron microscope images (HRTEM) are shown in Figure 5. No essential structural change is observed between the control VACNTs and the annealed VACNTs, while the degraded VACNTs show damaged walls. Reconstruction of CNTs is also observed in the overtreated sample: in contrast to the wall-to-wall distance of  $\sim 3.4$  Å in the CNTs, the reconstructed allotrope shows a much smaller interlayer distance,  $\sim 2.3$  Å, well matching the characteristic interlayer distance of hexagonal diamond or diamond-like carbon.<sup>59–62</sup> This indicates very high temperature and local pressure that the CNTs may experience in the microwave radiation. Large-scale reconstruction of the CNTs is not observed in our study, probably because the ultrafast heating process does not allow the large-scale reconstruction to take place kinetically.<sup>34</sup>

The high treatment temperature, ultrafast heating and strong interaction between the CNTs and the microwave field result in reduced defect density of the CNTs. First, CNTs are known to “store” hydrogen,<sup>63,64</sup> the C–H sites in the CNT structure can be healed up by outgassing of hydrogen under microwave irradiation.<sup>34,35</sup> Second, the oxidized sites formed in the as-synthesized CNTs may also have been partially reduced within short treatment duration. Recently, oxygen-containing functional groups introduced to CNTs at high temperatures during CNT synthesis have

been found to be unstable.<sup>65</sup> During the microwave treatment, the structural and the adsorbed hydrogen in the argon environment probably causes the local reduction/reconstruction of the oxygen-containing functional sites. This is the possible reason why water vapor was detected during CNT outgassing in the microwave field.<sup>34,35</sup> With extended microwave treatment duration, the “stored” hydrogen may have been depleted, rendering the CNTs subjective to oxidation. Although the temperature that the CNTs reach in the VFM may not be as high as that used for the conventional high-temperature thermal annealing for MWNTs, CNT annealing is still possible when we take into account the special role of microwave in dramatically increasing reaction rates and the capability of inducing chemical reactions which cannot proceed by thermal heating alone.<sup>66,67</sup> In addition, we note that a relatively low annealing temperature (700 °C) has been proved to be effective for CNT annealing by healing up the defective sites in CNT structures caused by acid treatment during CNT purification.<sup>42</sup>

To evaluate the mechanical properties of the CNTs, we prepared CNT fibers (10  $\mu\text{m}$  in diameter) on the basis of a twisting and densification spinning process and measured the tensile properties of the CNT fibers.<sup>68</sup> The experimental data are listed in Table 1. The fracture strength and the modulus of the CNT fibers made of the control VACNTs (CF1) are  $0.58 \pm 0.12$  and  $54.7 \pm 3.8$  GPa, respectively, comparable to the values for CNT fibers reported by other researchers.<sup>11,13,16,17,69–71</sup> It is evident that 3 min of VFM (500 W) treatment of the VACNTs improved dramatically the fracture strength and the modulus of the as-spun CNT fibers (CF2) up to  $0.79 \pm 0.08$  and  $89.3 \pm 22.1$  GPa, respectively. The high strength is almost comparable to the record strength of 1 GPa reported by Windle’s group<sup>12</sup> (with 20-mm gauge length of the tested specimens) but higher than Windle’s high-performance fibers (0.44 GPa) from dog-bone tubes.<sup>69</sup> The tensile strength is even comparable with the strength of superstrong CNT/polymer composite fibers (0.85 GPa).<sup>14,16</sup> In comparison, extended duration of microwave treatment degrades the CNTs (CF3).

The mechanical property results are consistent with the Raman, TGA, XPS, and TEM results except that the fibers from the degraded VACNTs possess higher strength and elastic modulus than those from the control VACNTs. A possible explanation is the enhancement in tube–tube anchoring force due to the increased number of polar groups on the CNT walls by the extended microwave treatment duration. Given the high packing density of CNTs in the spun fibers, we believe that interfacial stress transfer becomes a significant factor that determines the apparent collective Young’s modulus.<sup>72,73</sup> For the sake of comparison, we list, in Table 1, the mechanical properties of CNT fibers (CF4, 10  $\mu\text{m}$  in diameter) spun from VACNTs that are grown



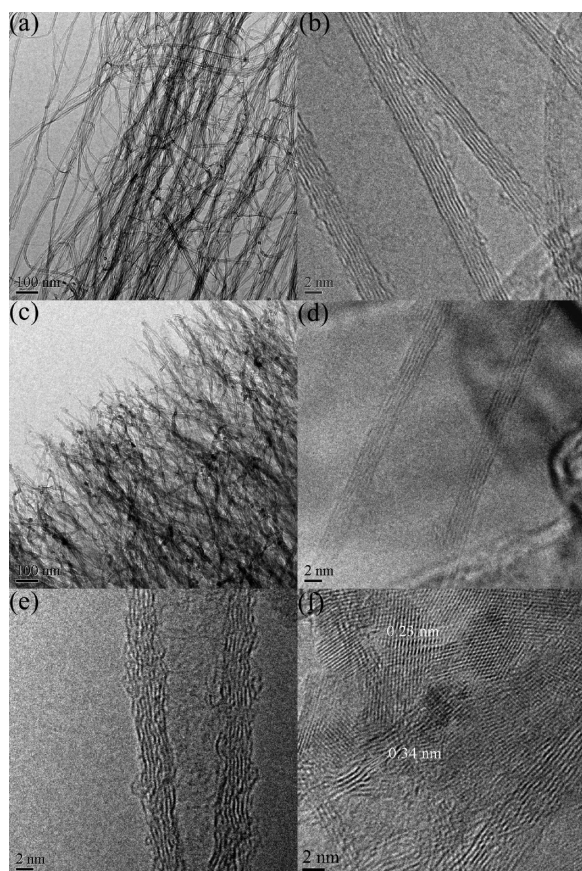


**Figure 5.** TEM images of the control VACNTs (a and b), the VACNTs treated by VFM with 500 W of power for 180 s (c and d) and the VACNTs treated by VFM with 500 W of power for 300 s (e and f). Image f shows the reconstruction of CNTs to form a different carbon allotrope observed in the overtreated sample.

**TABLE 1. Data of the Mechanical Properties for the CNT Fibers<sup>a</sup>**

	CF1	CF2	CF3	CF4
fracture strength (GPa)	0.58(0.12)	0.79(0.08)	0.63(0.14)	0.50(0.10)
elastic modulus (GPa)	54.7(3.8)	89.3(22.1)	73.5(7.3)	8.0(1.0)

<sup>a</sup>CF1, CF2, and CF3 represent the fibers spun from the control VACNTs, the VACNTs after 3 min of VFM (500 W) treatment, and those after 5 min of VFM (500 W) treatment, respectively; CF4 represents the fibers spun from VACNTs grown with the assistance of a trace amount of water rather than hydrogen peroxide.<sup>68</sup> The number in the brackets is the standard deviation.

with the assistance of a trace amount of water,<sup>68</sup> the as-synthesized VACNTs show nearly no surface functional groups.<sup>51</sup> In contrast, the control VACNTs used in this study are mildly surface functionalized by the hydrogen peroxide during the CVD process.<sup>51</sup> The fracture strength and modulus of CF1 are  $\sim 16\%$  and  $\sim 580\%$ , respectively, higher than those of CF4. Therefore, surface polar groups do account for the elastic modulus of the CNT fibers.

Besides the mechanical properties, we also measured the electrical conductivities of the CNT fibers. The electrical conductivity of CF1 and CF2 are  $6.9 \pm 0.7 \times 10^4$  and  $8.3 \pm 1.3 \times 10^4$  S m<sup>-1</sup>, respectively, also

indicating an effective CNT quality improvement after the microwave treatment. The high electrical conductivity is comparable to the highest-known value measured for a CNT assembly to date.<sup>74</sup> In comparison, the electrical conductivity of CF3 is much lower,  $\sim 2 \times 10^4$  S m<sup>-1</sup>. Illustration of the electrical conductivity measurement technique with effectively reduced contact resistance is included in the Supporting Information.

Finally, we would like to discuss briefly about CNT response in microwave radiation, of which the mechanism is still controversial today.<sup>40</sup> Wadhawan *et al.*<sup>35</sup> compared the microwave responses of raw and purified single-walled carbon nanotubes (SWNTs) and attributed the strong microwave absorption of the raw SWNTs to the high concentration of catalyst residue. In contrast, Imholt *et al.*<sup>34</sup> reported nearly no difference in the microwave response between raw and purified SWNTs. Recently, Naab *et al.*<sup>36</sup> found a fairly weak correlation between catalyst residue and microwave response of CNTs; instead, structural properties of CNTs seemed to play the key role. In our study, the VACNTs are pretty clean, with almost no or very little iron residue after they are peeled off the growth substrate.<sup>75</sup> The high purity of the VACNTs, as mentioned before, can also be seen from the TGA and HRTEM results. The free-standing VACNTs, however, show no distinct difference in microwave response compared to the on-substrate VACNTs. Thus, the response of CNTs in microwave is not determined by metal particle residue. We also notice that the VACNTs, before and after microwave annealing at varied duration (shorted than 3 min), show almost the same fast microwave response, which indicates a weak influence of structural defects on CNT response in microwave radiation.

So what is the key factor that determines the CNT response in a microwave field? Actually, we do observe some interesting phenomena, named “cloning of microwave response of CNTs” by us, which are summarized as follows: (1) the microwave response of the as-grown VACNTs—in terms of the capability of being fast heated in microwave radiation—coincides with that of the growth substrate; (2) after a VACNT array is peeled off the growth substrate, both the free-standing CNT array and the growth substrate retain their original responses to microwave; (3) each layer of VACNTs in a bilayer structure (synthesized using the method in ref 75) exhibits almost the same microwave response. Therefore, microwave response of CNTs seems to be an intrinsic property of the CNTs, which is directly determined by the microwave response of the growth substrate. The mechanism of CNT fast heating in microwave, thus, has become more complicated than what people have ever thought before. If, as Naab concluded and as we propose here, CNT structure is the dominating factor that determines its

microwave response, then how can we correlate the CNT structure to the microwave response of the growth substrate?

## CONCLUSIONS

An ultrafast microwave annealing process has been introduced to improve CNT quality and is important for CNT applications. The as-annealed CNTs showed

dramatic improvement in thermal stability, mechanical properties, and electrical conductivity. CNT response in microwave has been discussed and its mechanism seems to be more complicated than expected. We believe that the cloning phenomenon discovered in terms of microwave response of CNTs confers benefits in further understanding of CNT structure and the relation between CNT structure and catalyst particles.

## EXPERIMENTAL SECTION

VACNT arrays of 1 mm thick were synthesized by, as reported in previous publications,<sup>5,50–52</sup> a CVD process at 750 °C with gas flow rate ratio as Ar/H<sub>2</sub>/C<sub>2</sub>H<sub>4</sub> = 380/150/150 sccm and a small amount of Ar bubbled through H<sub>2</sub>O<sub>2</sub> (5 wt %) into the furnace chamber. A 7-nm-thick Al<sub>2</sub>O<sub>3</sub> support layer and a 2.2-nm-thick iron catalyst layer were deposited onto a thermally oxidized silicon substrate, sequentially and respectively, by atomic layer deposition (ALD) and e-beam evaporation. Introduction of ALD to preparing Al<sub>2</sub>O<sub>3</sub> is a noteworthy modification to the catalyst recipe used previously.<sup>10,76</sup> The significance of ALD in the support layer preparation has been discussed in details in a recent publication.<sup>77</sup>

Microwave treatment of the synthesized vACNTs was carried out in a variable-frequency microwave (VFM) chamber (MicroCure2100, Lambda Technologies) with the following parameters: 6.425 GHz (central frequency), 1.150 GHz (bandwidth), and 0.1 s (sweep time). The microwave system could be programmed to operate at different power levels and duration. Inside the microwave chamber was a self-setup argon-filled glass chamber, in which the VACNT samples were placed. Upon microwave radiation, intensive light emitting, fast heating, and outgassing were observed from the VACNT samples (Supporting Information). VFM techniques have the advantage of being capable of overcoming the nonuniformities in temperature and arcing associated with traditional microwave processing. In our study, 500 W microwave output was able to heat the VACNT samples above 400 °C within a few seconds. It has been found that such highly microwave-responsive CNTs could be fast-heated to “super” high temperatures (e.g., ~3000 K).<sup>38</sup> However, monitoring the actual temperature of the CNTs in the VFM chamber during microwave radiation is extremely challenging since infrared emissivity of CNTs especially at high temperatures is unknown.

**Acknowledgment.** The authors acknowledge NSF (0800849) and RCI at Rockwell Collins for financial support and Z. L. Wang and D. Bucknall at Georgia Institute of Technology for helpful discussion. J. Shang’s work is partly financially supported by National Science Foundation of China (No. 50775038), Project 863 (2009AA04Z306) and Project for talent person of new century by Education Ministry and Jiangsu Province of China.

**Supporting Information Available:** I<sub>b</sub>/I<sub>G</sub> of the VACNT samples treated by VFM with 100 and 300 W of power at varied duration, a video regarding the VACNT response to the microwave, and illustration of the electrical conductivity measurement technique. This material is available free of charge via the Internet at <http://pubs.acs.org>.

## REFERENCES AND NOTES

- Kreupl, F.; Graham, A. P.; Duesberg, G. S.; Steinhogel, W.; Liebau, M.; Unger, E.; Honlein, W. Carbon Nanotubes in Interconnect Applications. *Microelectron. Eng.* **2002**, *64*, 399–408.
- Li, J.; Ye, Q.; Cassell, A.; Ng, H. T.; Stevens, R.; Han, J.; Meyyappan, M. Bottom-Up Approach for Carbon Nanotube Interconnects. *Appl. Phys. Lett.* **2003**, *82*, 2491–2493.
- Nihei, M.; Kawabata, A.; Kondo, D.; Horibe, M.; Sato, S.; Awano, Y. Electrical Properties of Carbon Nanotube Bundles for Future via Interconnects. *Jpn. J. Appl. Phys., Part 1* **2005**, *44*, 1626–1628.
- Naeemi, A.; Sarvari, R.; Meindl, J. D. Performance Comparison between Carbon Nanotube and Copper Interconnects for Gigascale Integration (GSI). *IEEE Electron Device Lett.* **2005**, *26*, 84–86.
- Zhu, L. B.; Sun, Y. Y.; Hess, D. W.; Wong, C. P. Well-Aligned Open-Ended Carbon Nanotube Architectures: An Approach for Device Assembly. *Nano Lett.* **2006**, *6*, 243–247.
- Biercuk, M. J.; Llaguno, M. C.; Radosavljevic, M.; Hyun, J. K.; Johnson, A. T.; Fischer, J. E. Carbon Nanotube Composites for Thermal Management. *Appl. Phys. Lett.* **2002**, *80*, 2767–2769.
- Liu, C. H.; Huang, H.; Wu, Y.; Fan, S. S. Thermal Conductivity Improvement of Silicone Elastomer with Carbon Nanotube Loading. *Appl. Phys. Lett.* **2004**, *84*, 4248–4250.
- Huang, H.; Liu, C. H.; Wu, Y.; Fan, S. S. Aligned Carbon Nanotube Composite Films for Thermal Management. *Adv. Mater.* **2005**, *17*, 1652–1656.
- Xu, J.; Fisher, T. S. Enhancement of Thermal Interface Materials with Carbon Nanotube Arrays. *Int. J. Heat Mass Transfer* **2006**, *49*, 1658–1666.
- Cola, B. A.; Xu, J.; Chen, C. R.; Xu, X. F.; Fisher, T. T.; Hu, H. P. Photoacoustic Characterization of Carbon Nanotube Array Thermal Interfaces. *J. Appl. Phys.* **2007**, *101*, 054313.
- Vigolo, B.; Penicaud, A.; Coulon, C.; Sauder, C.; Paillet, R.; Journet, C.; Bernier, P.; Poulin, P. Macroscopic Fibers and Ribbons of Oriented Carbon Nanotubes. *Science* **2000**, *290*, 1331–1334.
- Koziol, K.; Vilatela, J.; Moissala, A.; Motta, M.; Cuniff, P.; Sennett, M.; Windle, A. High-Performance Carbon Nanotube Fiber. *Science* **2007**, *318*, 1892–1895.
- Motta, M.; Li, Y. L.; Kinloch, I.; Windle, A. Mechanical Properties of Continuously Spun Fibers of Carbon Nanotubes. *Nano Lett.* **2005**, *5*, 1529–1533.
- Miaudet, P.; Badaire, S.; Maugey, M.; Derre, A.; Pichot, V.; Launois, P.; Poulin, P.; Zakri, C. Hot-Drawing of Single and Multiwall Carbon Nanotube Fibers for High Toughness and Alignment. *Nano Lett.* **2005**, *5*, 2212–2215.
- Jiang, K. L.; Li, Q. Q.; Fan, S. S. Nanotechnology: Spinning Continuous Carbon Nanotube Yarns—Carbon Nanotubes Weave Their Way into a Range of Imaginative Macroscopic Applications. *Nature* **2002**, *419*, 801.
- Zhang, M.; Atkinson, K. R.; Baughman, R. H. Multifunctional Carbon Nanotube Yarns by Downsizing an Ancient Technology. *Science* **2004**, *306*, 1358–1361.
- Zhang, X. F.; Li, Q. W.; Tu, Y.; Li, Y. A.; Coulter, J. Y.; Zheng, L. X.; Zhao, Y. H.; Jia, Q. X.; Peterson, D. E.; Zhu, Y. T. Strong Carbon-Nanotube Fibers Spun from Long Carbon-Nanotube Arrays. *Small* **2007**, *3*, 244–248.
- Baughman, R. H.; Zakhidov, A. A.; de Heer, W. A. Carbon Nanotubes—The Route toward Applications. *Science* **2002**, *297*, 787–792.
- Barinov, A.; Gregoratti, L.; Dudin, P.; La Rosa, S.; Kiskinova, M. Imaging and Spectroscopy of Multiwalled Carbon Nanotubes during Oxidation: Defects and Oxygen Bonding. *Adv. Mater.* **2009**, *21*, 1916–1920.

20. Mielke, S. L.; Troya, D.; Zhang, S.; Li, J. L.; Xiao, S. P.; Car, R.; Ruoff, R. S.; Schatz, G. C.; Belytschko, T. The Role of Vacancy Defects and Holes in the Fracture of Carbon Nanotubes. *Chem. Phys. Lett.* **2004**, *390*, 413–420.
21. Sammakorpi, M.; Krashennikov, A.; Kuronen, A.; Nordlund, K.; Kaski, K. Mechanical Properties of Carbon Nanotubes with Vacancies and Related Defects. *Phys. Rev. B* **2004**, *70*, 8.
22. Yi, W.; Lu, L.; Zhang, D. L.; Pan, Z. W.; Xie, S. S. Linear Specific Heat of Carbon Nanotubes. *Phys. Rev. B* **1999**, *59*, R9015–R9018.
23. Hou, W. Y.; Xiao, S. P. Mechanical Behaviors of Carbon Nanotubes with Randomly Located Vacancy Defects. *J. Nanosci. Nanotechnol.* **2007**, *7*, 4478–4485.
24. Scarpa, F.; Adhikari, S.; Wang, C. Y. Mechanical Properties of Nonreconstructed Defective Single-Wall Carbon Nanotubes. *J. Phys. D* **2009**, *42*, 6.
25. Che, J. W.; Cagin, T.; Goddard, W. A. Thermal Conductivity of Carbon Nanotubes. *Nanotechnology* **2000**, *11*, 6569.
26. Liu, C. H.; Fan, S. S. Effects of Chemical Modifications on the Thermal Conductivity of Carbon Nanotube Composites. *Appl. Phys. Lett.* **2005**, *86*, 3.
27. Mingo, N.; Broido, D. A. Length Dependence of Carbon Nanotube Thermal Conductivity and the “Problem of Long Waves”. *Nano Lett.* **2005**, *5*, 1221–1225.
28. Padgett, C. W.; Brenner, D. W. Influence of Chemisorption on the Thermal Conductivity of Single-Wall Carbon Nanotubes. *Nano Lett.* **2004**, *4*, 1051–1053.
29. Monthieux, M.; Smith, B. W.; Burteaux, B.; Claye, A.; Fischer, J. E.; Luzzi, D. E. Sensitivity of Single-Wall Carbon Nanotubes to Chemical Processing: An Electron Microscopy Investigation. *Carbon* **2001**, *39*, 1251–1272.
30. Metenier, K.; Bonnamy, S.; Beguin, F.; Journet, C.; Bernier, P.; de La, Chapelle, M. L.; Chauvet, O.; Lefrant, S. Coalescence of Single-Walled Carbon Nanotubes and Formation of Multiwalled Carbon Nanotubes under High-Temperature Treatments. *Carbon* **2002**, *40*, 1765–1773.
31. Bom, D.; Andrews, R.; Jacques, D.; Anthony, J.; Chen, B. L.; Meier, M. S.; Selegue, J. P. Thermogravimetric Analysis of the Oxidation of Multiwalled Carbon Nanotubes: Evidence for the Role of Defect Sites in Carbon Nanotube Chemistry. *Nano Lett.* **2002**, *2*, 615–619.
32. Paton, K. R.; Windle, A. H. Efficient Microwave Energy Absorption by Carbon Nanotubes. *Carbon* **2008**, *46*, 1935–1941.
33. Salvétat, J. P.; Kulik, A. J.; Bonard, J. M.; Briggs, G. A. D.; Stockli, T.; Metenier, K.; Bonnamy, S.; Beguin, F.; Burnham, N. A.; Forro, L. Elastic Modulus of Ordered and Disordered Multiwalled Carbon Nanotubes. *Adv. Mater.* **1999**, *11*, 161–165.
34. Imholt, T. J.; Dyke, C. A.; Hasslacher, B.; Perez, J. M.; Price, D. W.; Roberts, J. A.; Scott, J. B.; Wadhawan, A.; Ye, Z.; Tour, J. M. Nanotubes in Microwave Fields: Light Emission, Intense Heat, Outgassing, and Reconstruction. *Chem. Mater.* **2003**, *15*, 3969–3970.
35. Wadhawan, A.; Garrett, D.; Perez, J. M. Nanoparticle-Assisted Microwave Absorption by Single-Wall Carbon Nanotubes. *Appl. Phys. Lett.* **2003**, *83*, 2683–2685.
36. Naab, F.; Dhoubhadel, M.; Holland, O. W.; Duggan, J. L.; Roberts, J.; McDaniel, F. D. In *The Role of Metallic Impurities in the Interaction of Carbon Nanotubes with Microwave Radiation*, 10th International Conference on Particle Induced X-ray Emission and its Analytical Applications, Portoroz, Slovenia, 2004; Wiley Interscience: Portoroz, Slovenia, 2004; pp 601.1–601.4.
37. Babaei, S.; Solari, M. S. Microwave Attenuation of Hydrogen Plasma in Carbon Nanotubes. *J. Appl. Phys.* **2008**, *104*, 124315.
38. Ye, Z.; Deering, W. D.; Krokhn, A.; Roberts, J. A. Microwave Absorption by an Array of Carbon Nanotubes: A Phenomenological Model. *Phys. Rev. B* **2006**, *74*, 075425.
39. Kim, J.; So, H. M.; Kim, N.; Kim, J. J.; Kang, K. Microwave Response of Individual Multiwall Carbon Nanotubes. *Phys. Rev. B* **2004**, *70*, 153402.
40. Vazquez, E.; Prato, M. Carbon Nanotubes and Microwaves: Interactions, Responses, and Applications. *ACS Nano* **2009**, *3*, 3819–3824.
41. Delgado, J. L.; De la Cruz, P.; Langa, F.; Urbina, A.; Casado, J.; Lopez Navarrete, J. T. Microwave-Assisted Sidewall Functionalization of Single-Wall Carbon Nanotubes by Diels–Alder Cycloaddition. *Chem. Commun.* **2004**, 1734–1735.
42. Wang, Y.; Iqbal, Z.; Mitra, S. Rapidly Functionalized, Water-Dispersed Carbon Nanotubes at High Concentration. *J. Am. Chem. Soc.* **2006**, *128*, 95–99.
43. Raghuvveer, M. S.; Agrawal, S.; Bishop, N.; Ramanath, G. Microwave-Assisted Single-Step Functionalization and *In Situ* Derivatization of Carbon Nanotubes with Gold Nanoparticles. *Chem. Mater.* **2006**, *18*, 1390–1393.
44. Brunetti, F. G.; Herrero, M. A.; de, M.; Munoz, J.; Giordani, S.; Diaz-Ortiz, A.; Filippone, S.; Ruaro, G.; Meneghetti, M.; Prato, P.; Va'zquez, E. Reversible Microwave-Assisted Cycloaddition of Aziridines to Carbon Nanotubes. *J. Am. Chem. Soc.* **2007**, *129*, 14580–14581.
45. Liu, J.; Zubiri, M. R. I.; Vigolo, B.; Dossot, M.; Fort, Y.; Ehrhardt, J. J.; McRae, E. Efficient Microwave-Assisted Radical Functionalization of Single-Wall Carbon Nanotubes. *Carbon* **2007**, *45*, 885–891.
46. Kakade, B. A.; Pillai, V. K. An Efficient Route towards the Covalent Functionalization of Single Walled Carbon Nanotubes. *Appl. Surf. Sci.* **2008**, *254*, 4936–4943.
47. Colomer, J. F.; Marega, R.; Traboulsi, H.; Meneghetti, M.; Tendeloo, G. V.; Bonifazi, D. Microwave-Assisted Bromination of Double-Walled Carbon Nanotubes. *Chem. Mater.* **2009**, *21*, 4747–4749.
48. Lin, W.; Zhang, R. W.; Moon, K. S.; Wong, C. P. Molecular Phonon Couplers at Carbon Nanotube/Substrate Interface to Enhance Interfacial Thermal Transport. *Carbon* **2010**, *48*, 107–113.
49. Economopoulos, S. P.; Pagona, G.; Yudasaka, M.; Iijima, S.; Tagmatarchis, N. Solvent-Free Microwave-Assisted Bingel Reaction in Carbon Nanohorns. *J. Mater. Chem.* **2009**, *19*, 7326–7331.
50. Zhu, L. B.; Hess, D. W.; Wong, C. P. Monitoring Carbon Nanotube Growth by Formation of Nanotube Stacks and Investigation of the Diffusion-Controlled Kinetics. *J. Phys. Chem. B* **2006**, *110*, 5445–5449.
51. Lin, W.; Xiu, Y. G.; Jiang, H. J.; Zhang, R. W.; Hildreth, O.; Moon, K. S.; Wong, C. P. Self-Assembled Monolayer-Assisted Chemical Transfer of *In Situ* Functionalized Carbon Nanotubes. *J. Am. Chem. Soc.* **2008**, *130*, 9636–9637.
52. Zhu, L. B.; Xiu, Y. H.; Hess, D. W.; Wong, C. P. Aligned Carbon Nanotube Stacks by Water-Assisted Selective Etching. *Nano Lett.* **2005**, *5*, 2641–2645.
53. Dresselhaus, M. S.; Dresselhaus, G.; Saito, R.; Jorio, A. Raman Spectroscopy of Carbon Nanotubes. *Phys. Rep.* **2005**, *409*, 47–99.
54. Curran, S. A.; Talla, J. A.; Zhang, D.; Carroll, D. L. Defect-Induced Vibrational Response of Multiwalled Carbon Nanotubes Using Resonance Raman Spectroscopy. *J. Mater. Res.* **2005**, *20*, 3368–3373.
55. de los Arcos, T.; Garnier, M. G.; Oelhafen, P.; Mathys, D.; Seo, J. W.; Domingo, C.; Garci-Ramos, J. V.; Sanchez-Cortes, S. Strong Influence of Buffer Layer Type on Carbon Nanotube Characteristics. *Carbon* **2004**, *42*, 187–190.
56. Pang, L. S. K.; Saxby, J. D.; Chatfield, S. P. Thermogravimetric Analysis of Carbon Nanotubes and Nanoparticles. *J. Phys. Chem.* **1993**, *97*, 6941–6942.
57. McKee, G. S. B.; Flowers, J. S.; Vecchio, K. S. Length and the Oxidation Kinetics of Chemical-Vapor-Deposition-Generated Multiwalled Carbon Nanotubes. *J. Phys. Chem. C* **2008**, *112*, 10108–10113.
58. Rinzler, A. G.; Liu, J.; Dai, H.; Nikolaev, P.; Huffman, C. B.; Rodriguez-Macias, F. J.; Boul, P. J.; Lu, A. H.; Heymann, D.; Colbert, D. T.; *et al.* Large-Scale Purification of Single-Wall Carbon Nanotubes: Process, Product, and Characterization. *Appl. Phys. A* **1998**, *67*, 29–37.



59. Bundy, F. P.; Kasper, J. S. Hexagonal Diamond—A New Form of Carbon. *J. Chem. Phys.* **1967**, *46*, 3437–3446.
60. Wang, Z. X.; Yu, G. Q.; Ruan, M. L.; Zhu, F. Y.; Zhu, D. Z.; Pan, H. C.; Xu, H. J. Studies of Hexagonal Diamond of Nanograin in Graphite Surface Produced by Ar<sup>+</sup> Ion Bombardment. *Acta Phys. Sin.* **2000**, *49*, 1524–1527.
61. Chen, L. Y.; Chau-Nan Hong, F. Diamond-like Carbon Nanocomposite Films. *Appl. Phys. Lett.* **2003**, *82*, 3526–3528.
62. Sarangi, D.; Godon, C.; Granier, A.; Moalic, R.; Gouillet, A.; Turban, G.; Chauvet, O. Carbon Nanotubes and Nanostructures Grown from Diamond-like Carbon and Polyethylene. *Appl. Phys. A* **2001**, *73*, 765–768.
63. Tang, Y. H.; Lin, L. W.; Guo, C. Hydrogen Storage Mechanism of Multiwalled Carbon Nanotube Bundles Studied by X-ray Absorption Spectra. *Acta Phys. Sin.* **2006**, *55*, 4197–4201.
64. Nikitin, A.; Li, X. L.; Zhang, Z. Y.; Ogasawara, H.; Dai, H. J.; Nilsson, A. Hydrogen Storage in Carbon Nanotubes through the Formation of Stable C–H Bonds. *Nano Lett.* **2008**, *8*, 162–167.
65. Kundu, S.; Wang, Y. M.; Xia, W.; Muhler, M. Thermal Stability and Reducibility of Oxygen-Containing Functional Groups on Multiwalled Carbon Nanotube Surfaces: A Quantitative High-Resolution XPS and TPD/TPR Study. *J. Phys. Chem. C* **2008**, *112*, 16869–16878.
66. Young, D. D.; Nichols, J.; Kelly, R. M.; Deiters, A. Microwave Activation of Enzymatic Catalysis. *J. Am. Chem. Soc.* **2008**, *130*, 10048–10049.
67. Kappe, C. O. Controlled Microwave Heating in Modern Organic Synthesis. *Angew. Chem., Int. Ed.* **2004**, *43*, 6250–6284.
68. Zhang, S.; Zhu, L.; Minus, M. L.; Chae, H. G.; Jagannathan, S.; Wong, C. P.; Kowalik, J.; Roberson, L. B.; Kumar, S. Solid-State Spun Fibers and Yarns from 1-mm Long Carbon Nanotube Forests Synthesized by Water-Assisted Chemical Vapor Deposition. *J. Mater. Sci.* **2008**, *43*, 4356–4362.
69. Motta, M.; Moiala, A.; Kinloch, I. A.; Windle, A. H. High Performance Fibres from “Dog Bone” Carbon Nanotubes. *Adv. Mater.* **2007**, *19*, 3721–3726.
70. Li, Y. L.; Kinloch, I. A.; Windle, A. H. Direct Spinning of Carbon Nanotube Fibers from Chemical Vapor Deposition Synthesis. *Science* **2004**, *304*, 276–278.
71. Ma, W. J.; Liu, L. Q.; Yang, R.; Zhang, T. H.; Zhang, Z.; Song, L.; Ren, Y.; Shen, J.; Niu, Z. Q.; Zhou, W. Y.; Xie, S. S. Monitoring a Micromechanical Process in Macroscale Carbon Nanotube Films and Fibers. *Adv. Mater.* **2009**, *21*, 603–608.
72. Lin, W.; Wong, C. P. Comment on “The Effect of Stress Transfer within Double-Walled Carbon Nanotubes upon Their Ability to Reinforce Composites”. *Adv. Mater.*, published online December 4, 2009, <http://dx.doi.org/10.1002/adma.200902189>.
73. Shim, B. S.; Zhu, J.; Jan, E.; Critchley, K.; Ho, S. S.; Podsiadlo, P.; Sun, K.; Kotov, N. A. Multiparameter Structural Optimization of Single-Walled Carbon Nanotube Composites: Toward Record Strength, Stiffness, and Toughness. *ACS Nano* **2009**, *3*, 1711–1722.
74. Tawfik, S.; O'Brien, K.; Hart, A. J. Flexible High-Conductivity Carbon-Nanotube Interconnects Made by Rolling and Printing. *Small* **2009**, *5*, 2467–2473.
75. Zhu, L. B.; Xu, J. W.; Xiu, Y. H.; Sun, Y. Y.; Hess, D. W.; Wong, C. P. Growth and Electrical Characterization of High-Aspect-Ratio Carbon Nanotube Arrays. *Carbon* **2006**, *44*, 253–258.
76. Lin, W.; Moon, K. S.; Wong, C. P. A Combined Process of *in Situ* Functionalization and Microwave Treatment to Achieve Ultrasmall Thermal Expansion of Aligned Carbon Nanotube–Polymer Nanocomposites: Toward Applications as Thermal Interface Materials. *Adv. Mater.* **2009**, *21*, 2421–2424.
77. Lin, W.; Zhang, R. W.; Moon, K. S.; Wong, C. P. Synthesis of High-Quality Vertically Aligned Carbon Nanotubes on Bulk Copper Substrate for Thermal Management, submitted for publication.